生物化学与生物物理进展 *Progress in Biochemistry and Biophysics*, 2006, 33(6): 567~573
www.pibb.ac.cn

PIBB

Two Conformations of Native *Pseudomonas aeruginosa* Apoazurin in Solution

ZHONG Jin[1,2], ZHANG Hong-Jie[1)*]

([1)]*Institute of Biophysics, The Chinese Academy of Sciences, Beijing* 100101, China;
[2)]*Department of Pharmacy, College of Life Science, Jilin University, Changchun* 130023, China)

Abstract The mechanism of complex unfolding process of *Pseudomonas aeruginosa* apoazurin is an arguing problem. Recent published results indicated that this problem could be resolved by hypothesizing two native conformations coexisting in solution. Urea-induced unfolding of apoazurin was investigated further using intrinsinc fluorescence and CD spectra. Equilibrium unfolding curves in urea could be depicted with an apparent two-state transition, but a biphase kinetic process. The fast unfolding process is finished within a few seconds as monitored by stopped-flow fluorescence intensity, whereas the slow process requires several hours for unfolding at high concentration of urea at room temperature. The m_u values for the fast and slow phases are 2.24 and 2.45 $kJ \cdot mol^{-1} \cdot M^{-1}$ respectively. The difference between their unfolding activation energy is 22 $kJ \cdot mol^{-1}$. The time-resolved fluorescence emission spectra as well as the circular dichroism spectra just after manual mixing of protein and denaturant could be simulated by superposition of the spectra of the native and fully unfolded protein with the same coefficient of 0.37. This strongly suggests the three-state mechanism with a partially unfolded intermediate on its pathway is inadequate. The hypothesis of two native conformations coexistence is a reasonable selection.

Key words *Pseudomonas aeruginosa* apoazurin, unfolding, fluorescence spectrum, circular dichroism (CD)

Azurin is a blue copper protein, functioning in electron-transfer chains of plants and bacteria. Its high-resolution crystal structures exist for holo, apo, metal-substituted and some mutant forms[1~17]. However, only for *Pseudomonas aeruginosa* apoazurin two distinct crystalline forms were observed, which co-crystallized in the ratio 1∶1 as hetero-dimers in the tetramer of the asymmetric unit[4]. Form 1 closely resembles the holo-protein lacking copper, which is considered as evidence for the rack mechanism of metal uptake[17]. Form 2 shows conformational differences in the region near the metal binding site, which is induced by the incorporation of a water molecule into this site. The results are of large shifts of His117 and its adjacent residues Phe114, Pro115 and Gly116 as well as a conformational change of the side chain in the nearby residue Met13. Similar rearrangements were also observed in His46 and its surrounding peptide structure (residues 8 to 10). Local conformational isomerization in solution has also been investigated by time-resolved phosphorescence at different pH values[18]. The non-exponential decay of the unique Trp48 phosphorescence was ascribed to at least two conformations of the protein with different structural rigidities in the vicinity of the Trp residue, which were suggested to arise from the protonization/deprotonization of His 35. Recently Hansen *et al.*[19] further reported that the complex of urea-induced unfolding of apoazurin might be due to the heteroconformations.

The irreversibility of denaturant-induced unfolding of *P. aeruginosa* apoazurin hindered the thorough investigation of its complex unfolding mechanism, i.e. an intermediate pathway or a multiple conformers-coexisting two-state pathway. In a previous report[20], detailed thermodynamic and kinetic analysis for an apoazurin mutant M121L, of which the folding process was fully reversible in urea solution, provided the unambiguous evidence supporting a multiple conformation-coexisting model. DSC measurement reported later provided further support

*Corresponding author . Tel: 86-10-64837257, Fax: 86-10-64872026,
E-mail: hjzhang@sun5.ibp.ac.cn
Received: January 11, 2006 Accepted: February 27, 2006

for that hypothesis[21]. There are two conformations, N_1 and N_2, with different thermal stabilities. Low stability conformation has a relatively low mole enthalpy and low unfolding transition temperature, and high stability conformation has a relatively high mole enthalpy and high thermal unfolding transition temperature. pH change could move the conformation distribution. In this report, intrinsic fluorescence spectra and circular dichroism(CD) spectra were employed to characterize the parallel unfolding mechanism of apoazurin.

1 Materials and methods

1.1 Materials

P. aeruginosa azurin was expressed in *E. coli* strain HMS174 (DE3)[22] and was purified as described previously[23]. Protein purity was checked by SDS page, using 15% polyacrylamide gels, respectively. The apoprotein was prepared by dialyzing the sample against 100 mmol/L thiourea (Sigma)[24] in 50 mmol/L sodium phosphate buffer pH 5.1 for 12 h after it was reduced by 10 mmol/L ascorbate (Merck). The chemical agents of sodium acetate (supper pure) and glycine were from Merck. Its purity was checked by UV spectra at 625 nm. Protein concentration was determined by absorption using an extinction coefficient $A_{280}^{1\%}$= 6.31.

1.2 Fluorescence measurements

Fluorescence emission spectra were measured in 1 cm cells using a Spex Fluoromax spectrophotometer. Emission spectra were excited at 280 nm and recorded from 300 to 400 nm with an increment of 1 nm and a response time of 1 s. Excitation and emission slits of 5 nm each were employed during all spectra measurements. The slow unfolding kinetics was also monitored in the Spex Fluoromax spectrophotometer using manual mixing in a 3 ml cuvette and spectral line width of 2.6 nm.

The fast unfolding kinetics was monitored with a SFM-3 stopped-flow from Bio-Logic. The samples were excited at 280 nm and the emission above 305 nm was detected using a wavelength cut-off filter. A dead-time of 10.8 ms resulted from the conditions selected.

1.3 Circular dichroism measurements

CD measurements were performed using a Jobin Yvon CD6 spectropolarimeter. Spectra were averaged over 5 scans each made in the range from 190 to 260 nm. A 0.01 cm cuvette was employed and the spectra were corrected for the buffer signal. Ellipticity readings were converted into mean residue ellipticity values, $[\Theta]_{MRE}$, by the formula

$$[\Theta]_{MRE}=\frac{\Theta M}{10cdn} \quad (1)$$

where Θ is the measured ellipticity in millidegrees, M is the molecular mass of the apoazurin (13 929 Dalton), c is the concentration in mg·ml^{-1}, d is the path-length of the cuvette in cm, and n_r = 128 is the number of amino acid residues of azurin.

Slow unfolding kinetics was monitored at 219 nm in a 1 mm cuvette. The dead-time for manual mixing was about 60 s.

1.4 Data analysis

The digitized kinetic traces for the fast and slow unfolding processes were analyzed with equations (2) and (3), respectively.

$$F_t=(F_0-F_{f,\infty})\exp(-k_{u,f}t)+F_{f,\infty} \quad (2)$$

$$F_t=(F_0-F_{f,\infty}-F_{s,\infty})\exp(-k_{u,s}t)+F_{s,\infty} \quad (3)$$

where F_t, $F_{f,\infty}$ and $F_{s,\infty}$ are, respectively, the signal at time t, and the signals of the final states for the fast and slow processes. F_0 is the initial signal at time of zero. $k_{u,f}$ and $k_{u,s}$ is the unfolding kinetic constants for the fast and slow processes, respectively.

The free energies of activation for the unfolding ($\Delta G_u^{0\neq}$) were calculated using transition state theory according to Eyring

$$\ln k_u(H_2O)=\ln\frac{\kappa k_b T}{h}-\frac{\Delta G_u^{0\neq}(H_2O)}{RT} \quad (4)$$

where k_b is the Boltzmann constant, T is the absolute temperature in Kelvin, h is the Planck constant, R is the gas constant, and κ is the transmission factor which is arbitrarily set to unity.

Plots of $\ln k_u$ versus the concentrations of denaturant are linear in the post transition region, $\ln k_u(H_2O)$ could be linear extrapolated to the zero concentration of denaturant according to

$$\ln k_u=\ln k_u(H_2O)+m_u[\text{denaturant}] \quad (5)$$

2 Results

2.1 Urea-induced isothermal unfolding of apoazurin

Azurin contains one tryptophan, Trp 48, deeply buried in a hydrophobic core with maximum emission intensity at 308 nm in its native state. When the protein is unfolded, the maximum emission wavelength moves to 355 nm. Figure 1 shows urea unfolding curves, which were determined at pH 5.1. The transition at 20℃ after 48 h incubation time could be analyzed as one single sigmoidal transition with the midpoint of

urea concentration of about 5.7 mol/L (Figure 1). Refolding of the urea-denatured apoazurin is very slow. It took 26 days to accomplish complete refolding only at low urea concentrations (data not shown). The samples unfolded at 20℃ were incubated for 24 h at 40℃ and measured again. The result is also shown in Figure 1. In this case, a transition midpoint of 4.1 mol/L urea was observed. Obviously, at high temperature, apoazurin becomes less stable than at room temperature.

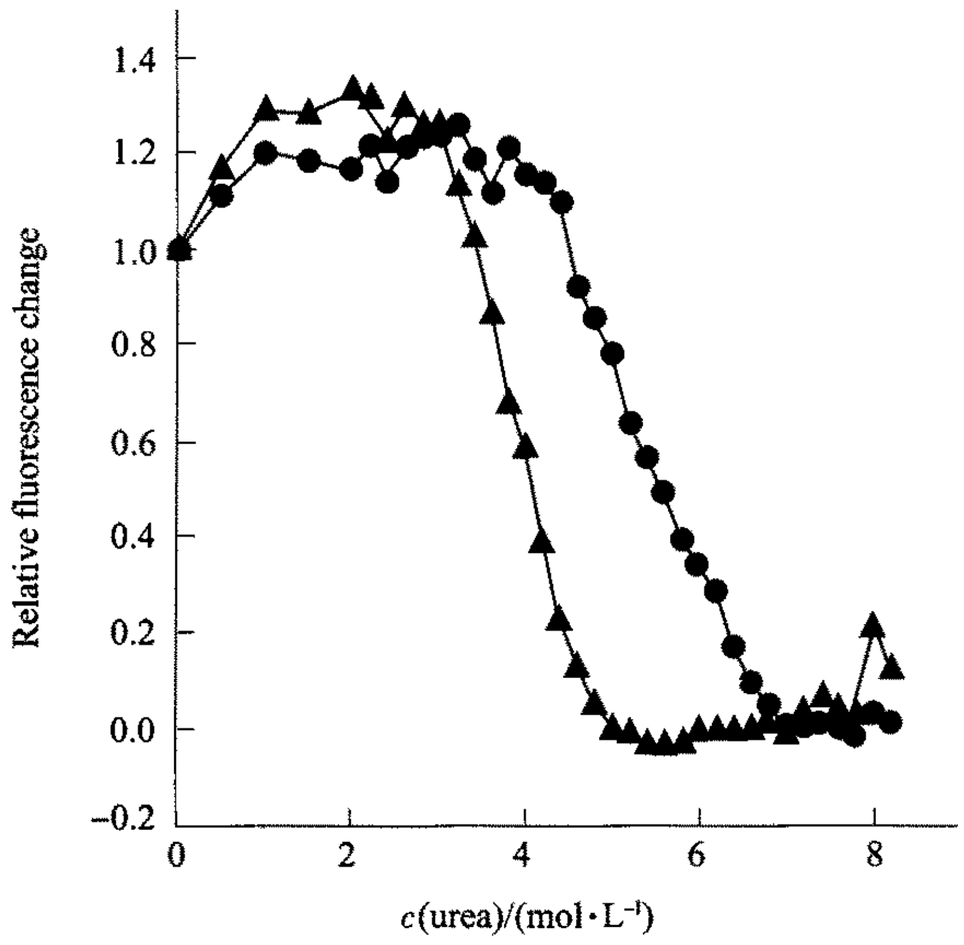

Fig. 1 Urea denaturation curves of apoazurin detected by fluorescence at 308 nm

Protein concentration was 0.005 g/L in 20 mmol/L NaOAc-HOAc, 1 mmol/L EDTA, pH 5.1 buffer solution. Excitation: 280 nm, cell: 1 cm optical path length. The slits for excitation and emission were both 5 nm. Circles show the results after 48 h incubation at 20℃, triangles that after incubation at 40℃ for another 24 h.

2.2 Unfolding kinetics monitored by fluorescence

Isothermal apoazurin unfolding kinetics in urea is characterized by a fast phase, sharing 63% signal change within the manual mixture time, and a very slow phase for the other 37% signal change when monitored by manual mixing fluorescence emission intensity at 308 nm (see below). The significant difference in rate constants makes it possible to follow separately the time-resolved fluorescence emission spectrum. Figure 2 shows the fluorescence spectrum at that moment when conformation N_1 has just unfolded (fast unfolding species, 63% of total protein) and N_2, the slow unfolding species, is still native. The spectra of the native and fully denatured protein are also shown in that graph. One remarkable characteristic of these spectra is the occurrence of an iso-emission point at about 347 nm, which can be considered as an indication of the occurrence of a two-state transition. The term "Two-state transition" means that during the equilibrium unfolding only 2 species, native and unfolded protein, occur. Another interesting feature is the following. The time-resolved fluorescence emission spectrum can be reconstructed from the native and fully unfolded spectra by linear superposition of two time-independent fluorescence spectra, using a weighting factor 0.37 for the conformation of the slow folding species N_2 in its native state and a factor of 0.63 for the fraction in the native state of the fast-unfolding species N_1. Only one assumption enters the simulation: The fluorescence spectra of both the native and unfolded states of N_1 and N_2 are identical. This assumption implies that the difference in native state conformations of N_1 and N_2 has no influence on the fluorescence spectrum of the protein. If one accepts this reasonable assumption, the fluorescence results on the unfolding kinetics suggest that apoazurin does not form characteristic unfolding intermediates but exhibits two-state unfolding of two native conformations.

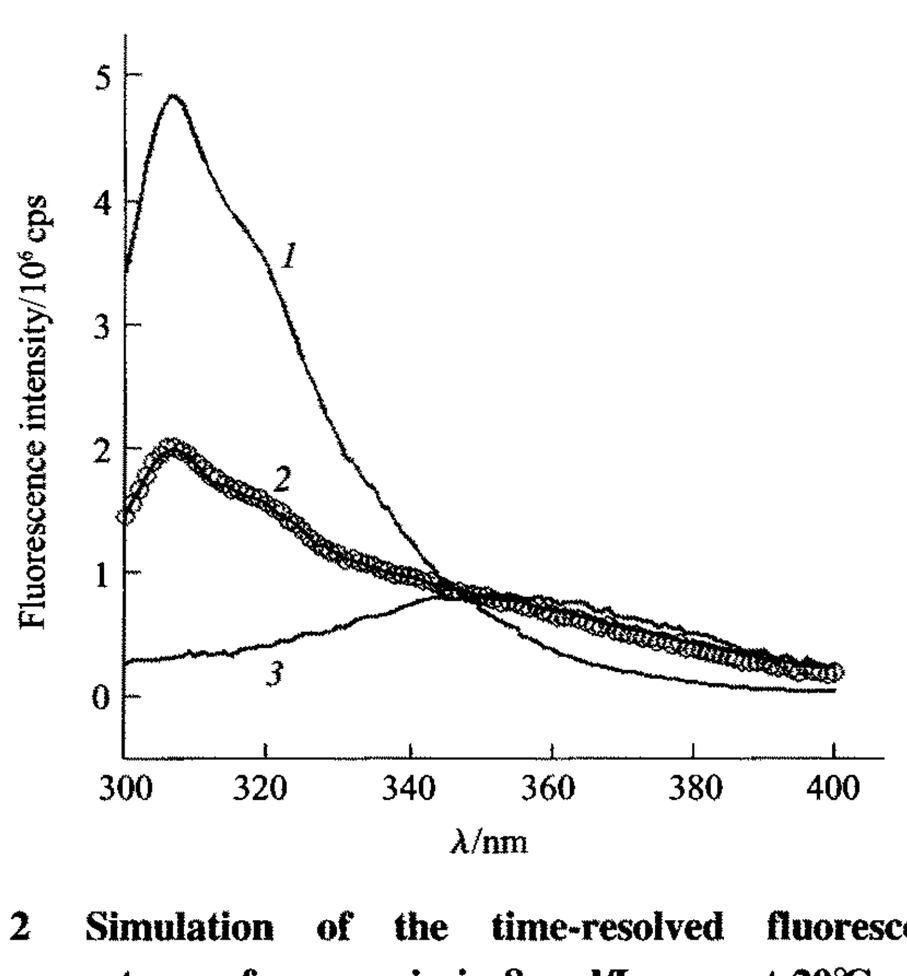

Fig. 2 Simulation of the time-resolved fluorescence spectrum of apoazurin in 8 mol/L urea at 20℃

Lines *1*, *2* and *3* are respectively the fluorescence spectra of native apoazurin, time-resolved in 8 mol/L urea just after unfolding of the fast species and of fully unfolded apoazurin in 8 mol/L urea. The simulated spectrum (circles) was calculated using 0.37×[native spectrum]+0.63×[unfolded spectrum]. Here [spectrum] represents the data set of the fluorescence intensity versus wavelength, and the coefficients 0.37 and 0.63 refer to the fractions of conformation N_1 and N_2, respectively, as observed in the kinetic unfolding measurement. Protein concentration was 0.005 g/L in 20 mmol/L NaOAc-HOAc, 1 mmol/L EDTA buffer solution at pH 5.1. Fluorescence was at 280 nm and the emission spectra were recorded from 300 nm to 400 nm. The slits for excitation and emission were both set to 5 nm.

The unfolding rate constants of the two hetero-conformations were also analyzed. The panel A in Figure 3 shows the fast process at 20℃. The total change in fluorescence emission intensity in 8.075 mol/L urea at wavelengths above 305 nm was monitored as a function of time. The data could be fitted to a single exponential equation with an unfolding rate constant of $k_{u,f} = 0.65\ s^{-1}$. The effect of urea concentration on the unfolding rate constants is shown in Figure 4. It is evident that the plot of $\ln k_{u,f}$ *versus* urea concentration is a straight line with the slope, $m_{u,f}$, of (2.24±0.16) kJ·mol^{-1}·M^{-1}. Thus $k_{u,f}$ can be calculated at any given urea concentration. Extrapolation to zero urea concentration according to equation. (4) yields the $k^0_{u,f}$ value in water as $(3.4 \pm 1.3) \times 10^{-4}\ s^{-1}$. Correspondingly the unfolding activation energy was calculated as 91 kJ·mol^{-1}.

Figure 3b shows the slow unfolding kinetics by employing manual mixing in 8.5 mol/L urea, 20℃. Within the dead-time of mixing, 63% of expected fluorescence intensity change at 308 nm has occurred. The data for the slow transition could also be fitted to a single exponential equation with a first order rate constant of $1.94 \times 10^{-4}\ s^{-1}$. The effect of urea concentration on the slow unfolding rate constant was also measured, as seen in Figure 4. As for the slow reaction, $\ln k_{u,s}$ depends linearly on urea concentration with a slope of $m_{u,s}$ (2.45 ±0.04) kJ·mol^{-1}·M^{-1}. Increasing the urea concentration leads also in this case to an increase in the unfolding rate constant. This finding suggests that the slow unfolding phase N_2 is caused by direct unfolding of a separate conformation, not by the conversion of N_2 to N_1. Its unfolding rate constant in water is $3.7 \times 10^{-8}\ s^{-1}$. Correspondingly the unfolding activation energy was determined as 113.5 kJ·mol^{-1}. The parameters for both of the fast and slow processes are tabulated in Table 1.

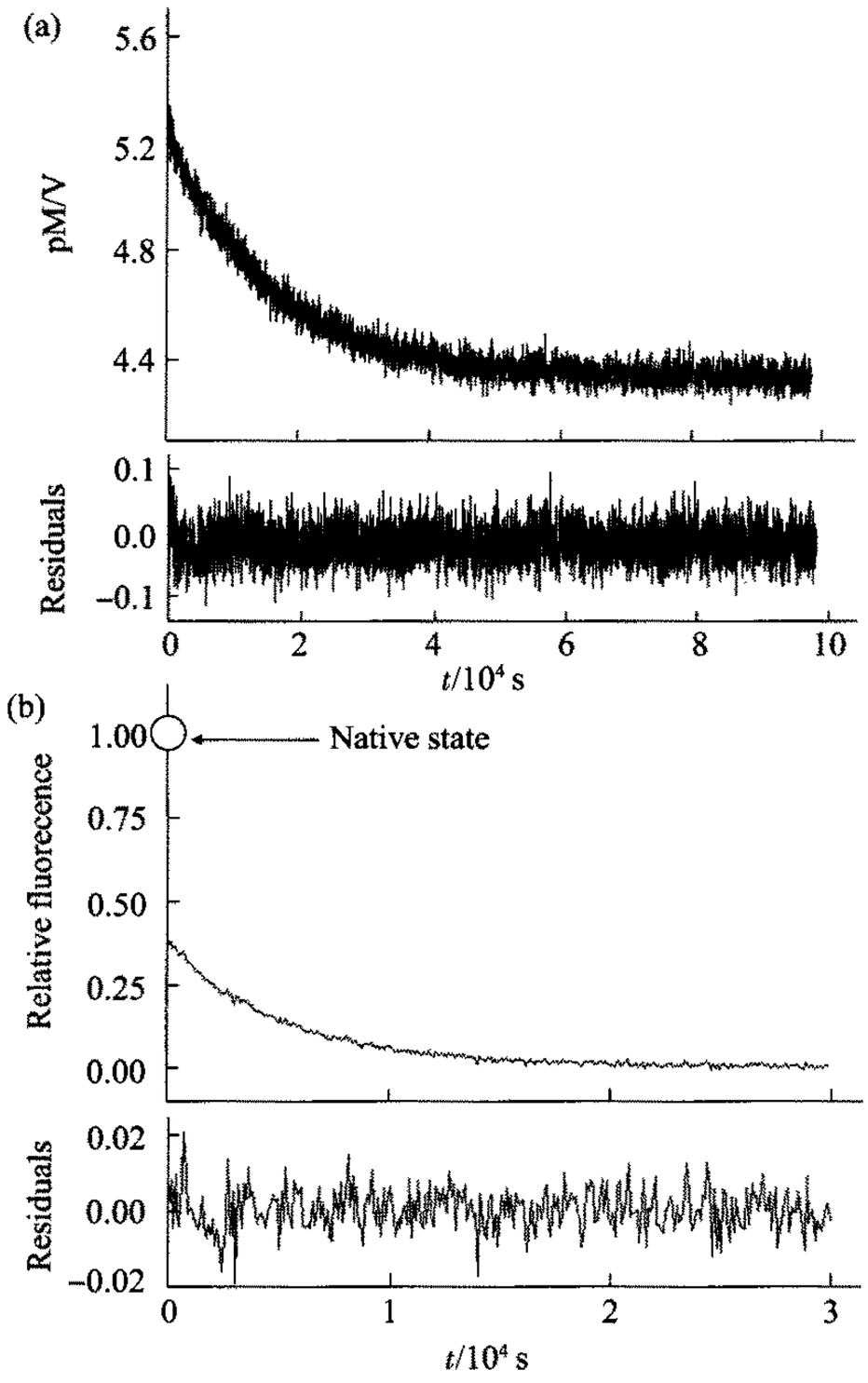

Fig. 3 Unfolding kinetics of apoazurin at pH 5.1, 20℃

(a) The fast unfolding process in 8.075 mol/L urea as detected by stopped-flow fluorescence with the filter-cutting off below 305 nm. The protein concentration was 0.014 g/L. (b) The slow process detected by fluorescence at 308 nm in 8.5 mol/L urea. The protein concentration was 0.005 g/L.

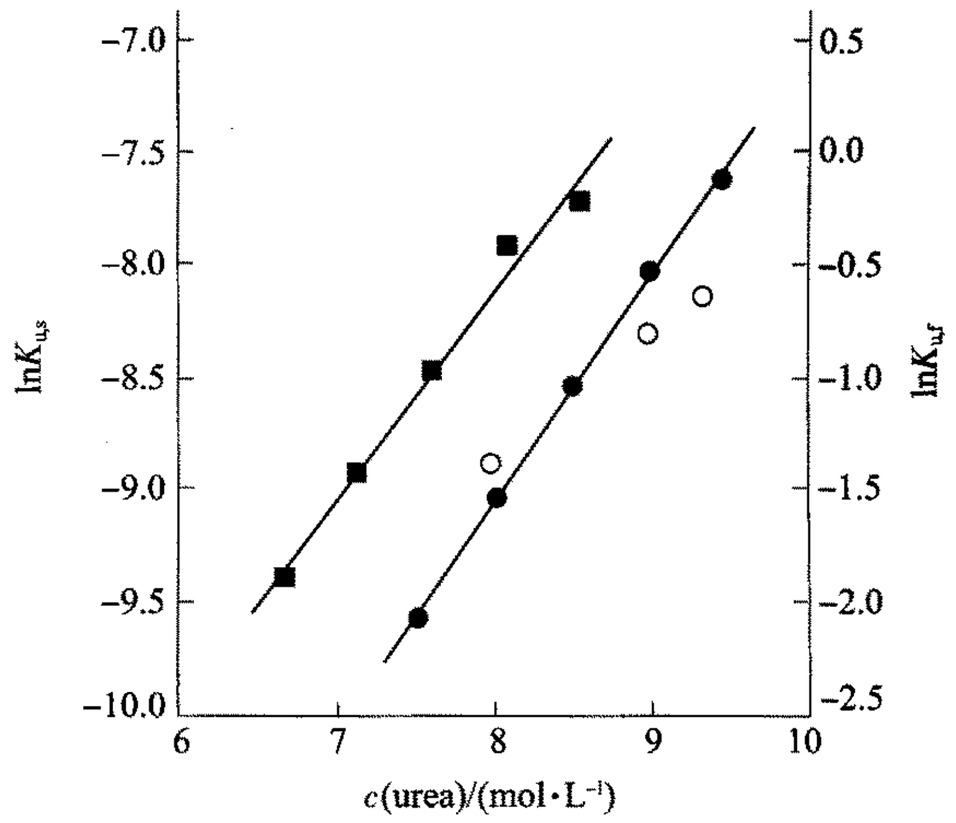

Fig. 4 Unfolding rate constants of apoazurin versus urea concentrations at pH 5.1, 20℃ monitored by fluorescence (filled) and CD (hollow), respectively

Squares indicate the fast unfolding process, and circles the slow process. The protein concentration was of 0.005 g/L for fluorescence measurements involving manual mixing, 0.014 g/L for stopped-flow fluorescence measurements, and 0.12 g/L for CD measurement (see Figure 6). The data were linearly fitted to equation (5).

Table 1. Kinetic parameters for the fast and slow unfolding of wt apoazurin

	m_u (kJ·mol^{-1}·M^{-1})	$k^0_u(H_2O)$ (s^{-1})	$\Delta G^{0\neq}_u(H_2O)$ (kJ·mol^{-1})
Fast phase	2.24±0.16	(3.4±1.3)×10^{-4}	91.18±1.21
Slow phase	2.45±0.04	(3.7±0.4)×10^{-8}	113.45±0.45

(T = 20℃)

2.3 Unfolding kinetics monitored by CD

Because fluorescence monitors in some cases only the local conformational change, the change in CD signal change at 219 nm was also be followed, which probes the change in secondary structure. Within the dead time of manual mixing, the large signal increase was observed, which was then followed by a rather slow signal increase, suggesting biphasic unfolding process (Figure 5). In analogy to the treatment of the fluorescence data, the CD spectrum observed just after the end of the fast unfolding process in 8 mol/L urea could be simulated using the same weighting factor of 0.37 for N_2 in the native state. The simulation is in excellent agreement with the measured spectrum as shown in Figure 6. Again we assume the same CD spectra for N_1 and N_2 in the native and the unfolded states, respectively. The dependence of the CD-based rate constant on urea concentration is also shown in Figure 4. It is evident that only the slow process is monitored by CD. The slope of the line connecting the three data points is somewhat lower than that observed with fluorescence measurements. However, the absolute values of the rate constants are in fair agreement with those measured by fluorescence.

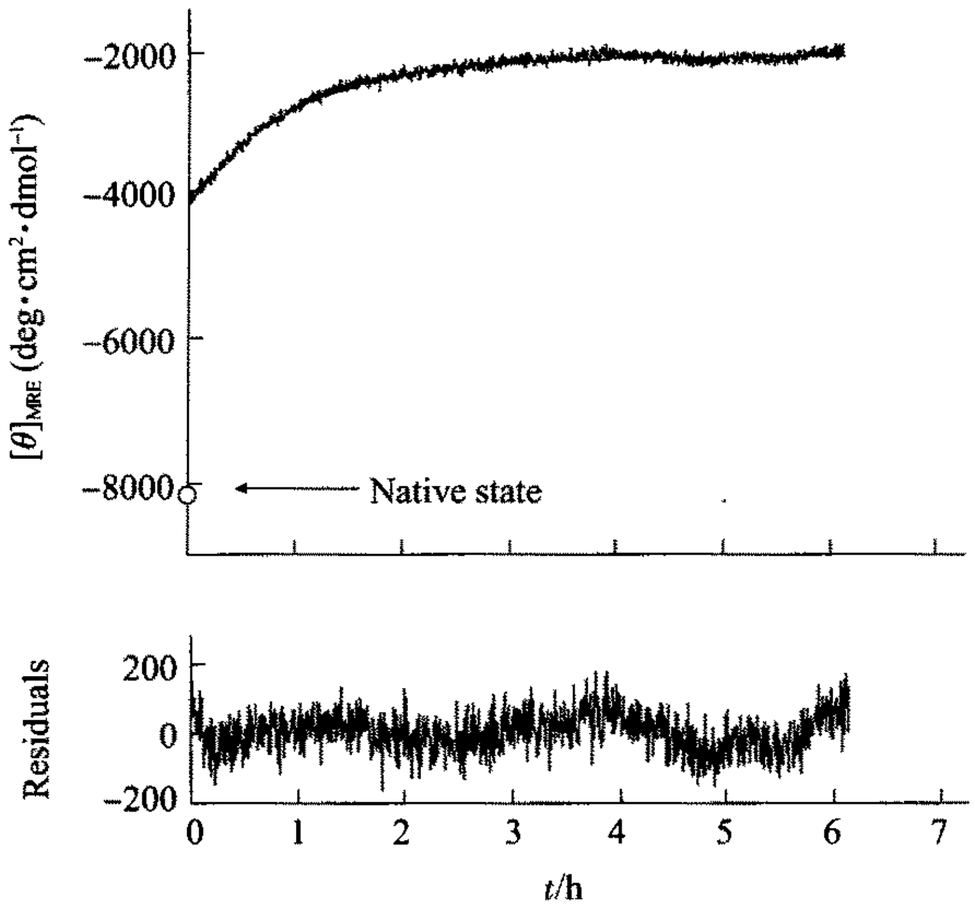

Fig. 5 Slow unfolding kinetics of apoazurin monitored by CD at 219 nm in 8 mol/L urea at 20℃

The protein and denaturant were manually mixed and CD signal was determined using a cuvette with a 1 mm light path. The dead time of manual mixing was about 60 s.

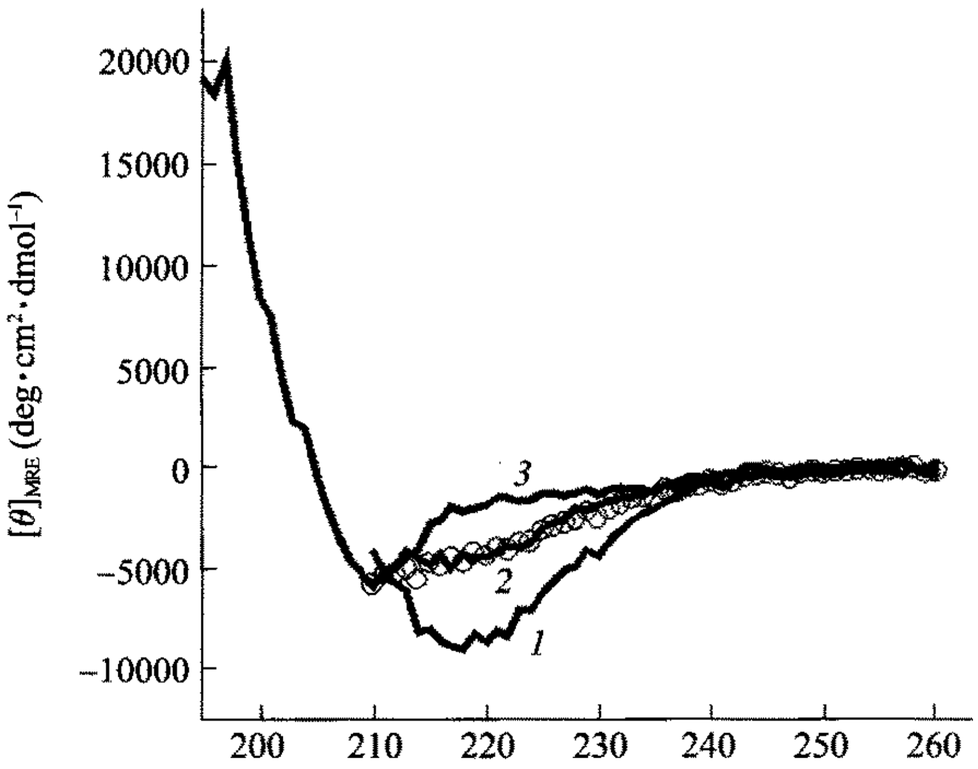

Fig. 6 Simulation of the time-resolved CD spectrum in 8 mol/L urea

The native (line *1*), time-resolved (line *2*) just after manual mixing with denaturant and fully unfolded (line *3*) CD spectra in 8 mol/L urea were measured separately. The intermediate spectrum during the unfolding process can be simulated using the equation 0.37×[native spectrum]+ 0.63×[unfolded spectrum]. Here [spectrum] represents the data set of a CD spectrum taken at time *t*, and the coefficients 0.63 and 0.37 are, respectively, the fractions of the conformation N_1 and N_2, that resulted from fitting of the kinetic unfolding curve to two synchronous first order processes. The protein concentration was 0.12 g/L in 20 mmol/L NaOAC-HOAc, 1 mmol/L EDTA buffer at pH 5.1.

3 Discussion

The complex unfolding of *P. aeruginosa* apoazurin had been documented extensive. One opinion is that this complex is a representation of the three-state unfolding pathway with a kinetic and/or stable intermediate, which was arbitrarily ascribed to unfolding of the α-helix subdomain, comprising of 28 aminio acids [22,25,26]. Clearly if it were correct, the secondary structure of the intermediate should contain only β-sheet structure, which could only provide a weak negative CD peak with the maximum wavelength at 215 nm, not at 219 nm. In a previous report using apoazurin mutant M121L [20], the incorrectness of the three-state unfolding mechanism with an intermediate has been analysized. In this report, both the fluorescence emission spectrum and CD spectrum of the state with first phase unfolding just finished could be reconstructed by a linear combination of the native and fully unfolded spectra with the same coefficients. Clearly the complex unfolding of *P. aeruginosa* apoazurin can't be ascribed to the existence of a partially folded intermediate on it unfolding pathway. As it has been done in the previous papers [20, 21], the two species are not due to the metal contamination. Only the two conformation coexistence hypothesis is adequate. With this concept in mind, many conflicted experimental results reported before could be interpreted well very.

This study also provides the structural information of each conformation. The hypothesis of

the same fluorescence emission spectra and CD spectra for both conformations indicated that the 3D structures for each conformation are very similar to each other. The m_u values, which are considered as the changes of the solvent access surface areas of the unfolding transition states [20], are also very close to each other, indicating that the transition state for each conformation is very similar. The difference is mainly on the unfolding activation energy barrels, which could be estimated as 22 kJ·mol^{-1}. This information provides clues to correlate the native conformations of apoazurin with the crystalline structures.

There were two apoazurin forms co-crystallized. In form 2 there were four hydrogen bonds among the incorporated water molecule and residues of Gly^{45} O, His^{46} Nδ, Cys^{112} Sγ and His^{117} Nδ, which ligate to copper in the holoprotein. From energy view hydrogen bond has less effect on protein stability than hydrophobic interaction, as its high energy is, at least in part balanced by the new hydrogen bond in its unfolding state. However in the transition state, where the hydrogen bonds caused by solvent hydration have not formed, the hydrogen bonds among the incorporated water and amino acid residues should strongly increase the unfolding activation energy. Hence it is rational to correlate the less stable conformation N_1 as apoform 1 and the stable conformation N_2 as apoform 2. This correlation could interpret the published data [20,21] well. Although the hydrogen bond effect is addressed here, it does not mean that it is the sole factor to make the large difference between their unfolding activation energy. The large arrangement of some residues, e.g. His117 etc, can also move its transition state. Unfortunately it is not clear whether they increase or decrease the transition state energy.

The fact of the argument on unfolding mechanism for so long reflects the importance of forming some methodologies to distinguish between intermediate model and multiple conformation coexistence models. For denaturant-induced unfolding process, one characteristic of the two-state transition is that the spectra in different denaturant concentrations share an isosbestic or isodichroic point [27]. Another version for this understanding is that the spectrum in each state can be simulated by linear summation using the native and fully unfolded protein spectra. If protein unfolds with two step transition while the middle state has its characteristic spectrum, the unfolding mechanism with an intermediate on/off its pathway can be drawn firmly; otherwise, the possibility of multiple conformation mechanism must be considered. From kinetic view if unfolding gives more than one relaxation phase, the time-resolved spectrum should be recorded. If this time-resolved spectrum can be simulated from that of native and denatured state, similarly, parallel unfolding mechanism caused by multiple conformation coexistence should be checked.

References

1 Adman E T, Jensen L H. Structural features of azurin at 2.7 Å resolution. Isr J Chem, 1981, **21** (1): 8～13

2 Nar H, Messerschmidt A, Huber R, *et al*. X-ray crystal structure of the two site-specific mutants His35Gln and His35Leu of azurin from *Pseudomonas aeruginosa*. J Mol Biol, 1991, **218** (2): 427～447

3 Nar H, Messerschmidt A, Huber R, *et al*. Crystal structure analysis of oxidized *Pseudomonas aeruginosa* azurin at pH 5.5 and pH 9.0. a pH-induced conformational transition involves a peptide bond flip. J Mol Biol, 1991, **221** (3): 765～772

4 Nar H, Messerschmidt A, Huber R, *et al*. Crystal structure of *Pseudomonas aeruginosa* apoazurin at 1.85 Å resolution. FEBS Lett, 1992, **306** (2～3): 119～124

5 Nar H, Huber R, Messerschmidt A, *et al*. Characterization and crystal structrue of zinc azurin, a by-product of heterologous expression in *Escherichia coli* of *Pseudomonas aeruginosa* copper azurin. Eur J Biochem, 1992, **205** (3): 1123～1129

6 Moratal J M, Romero A, Salgado J, *et al*. The crystal structure of Nickel(II)-Azurin. Eur J Biochem, 1995, **228** (3): 653～657

7 Bonander N, Vanngård T, Tsai L C, *et al*. The metal site of *Pseudomonas aeruginosa* azurin, revealed by a crystal structure determination of the Co (II) derivative and co-EPR spectroscopy. Proteins: Struct Funct Genet, 1997, **27** (3): 385～394

8 Sjölin L, Tsai L C, Langer V, *et al*. Structure of *Pseudomonas aeruginosai* zinc azurin mutant Asn47Asp at 2.4 Å resolution. Acta Cryst, 1993, **D49** (5): 449～457

9 Tsai L C, Bonander N, Harata K, *et al*. Mutant Met121Ala of *Pseudomonas aeruginosa* azurin and its azide derivative: crystal structures and spectral properties. Acta Cryst, 1996, **D52** (5): 950～958

10 Hammann C, Messerschmidt A, Huber R, *et al*. X-ray crystal structure of the two site-spicific mutants Ile7Ser and Phe110Ser of azurin from *Pseudomonas aeruginosa*. J Mol Biol, 1996, **255** (3): 362～366

11 Hammann C, van Pouderoyen G, Nar H, *et al*. Crystal structures of modified apo-His117Gly and apo-His46Gly mutants of *Pseudomonas aeruginosa* azurin. J Mol Biol, 1997, **266** (2): 357～366

12 Faham S, Mizoguchi T J, Adman E T, *et al*. Role of the active-site cysteine of *Pseudomonas aeruginosa* azurin. Crystal structure analysis of the Cu^{II}(Cys112Asp) protein. J Biol Inorg Chem, 1997, **2** (4): 464～469

13 Karlsson B G, Tsai L C, Nar H, *et al*. X-ray structure determination and characterizaton of the *Pseudomonas aeruginosa* azurin mutant Met121Glu. Biochemistry, 1997, **36** (14): 4089～4095

14 Messerschmidt A, Prade L, Kroes S J, *et al*. Rack-induced metal binding vs. flexibility: Met121His azurin crystal structures at different pH. Proc Natl Acad Sci USA, 1998, **95** (7): 3443～3448

15 Romero A, Hoitink C W G, Nar H, *et al*. X-ray analysis and spectroscopic characterization of M121Q azurin: A copper site model for stellacyanin. J Mol Biol, 1993, **229** (4): 1007～1021

16 Baker E N, Anderson B F, Blackwell K E, *et al*. The relative rigidity of the type Ⅰ copper site in azurin, as seen in high resolution X-ray analyses of various forms of the protein. J Inorg Biochem, 1991, **43** (2～3): 162

17 Shepard W E B, Anderson B F, Lewandoski D A, *et al*. Copper coordination geometry in azurin undergoes minimal change on reduction of copper(Ⅱ) to copper(Ⅰ). J Am Chem Soc, 1990, **112** (21): 7817～7819

18 Hansen J E, Steel D G, Gafni A. Detection of a pH-dependent conformational change in azurin by time resolved phosphorescence. Biophysical J, 1996, **71** (4): 2138～2143

19 Hansen J E, McBrayer M K, Robbins M, *et al*. A pH dependence study on the unfolding and refolding of apoazurin: comparison with Zn(Ⅱ) azurin. Cell Biochem Biophys, 2002, **36** (1): 19～40

20 Zhang H J. Conformational heterogeneity of apoazurin mutant M121L from *Pseudomonas aeruginosa*: A fluorescence study. Acta Biophysics Sinica, 2004, **20** (4): 275～284

21 Zhang H J. The thermodynamic evidence of two native conformations coexisting in solution for apoazurin: a DSC and CD study. Prog Biochem Biophys, 2005, **32** (3): 239～244
张洪杰. 生物化学与生物物理进展, 2005, **32** (3): 239～244

22 Engeseth H R, McMillin D R. Studies of thermally induced denaturation of azurin and azurin derivatives by differential scanning calorimetry: evidence for copper selectivity. Biochemistry, 1986, **25** (9): 2448～2455

23 Germanas J P, Di Bilio A J, Gray H B, *et al*. Site saturation of the histidine-46 position in *Pseudomonas aeruginosa* azurin: characterization of the His46Asp copper and cobalt proteins. Biochemistry, 1993, **32** (30): 7698～7702

24 Blaszak J A, McMillian D R, Thornton A T, *et al*. Kinetics of copper (Ⅱ) uptake by apoazurin in complexing media. J Biol Chem, 1983, **258** (16): 9886～9892

25 Leckner J, Bonander N, Wittung-Stafshede P, *et al*. The effect of the metal ion on the folding free energies of azurin: a comparison of the native, zinc and apoprotein. Biochim Biophys Acta, 1997, **1342** (1): 19～27

26 Malmström B G, Wittung-Stafshede P. Effects of protein folding on metalloprotein redox-active sites: electron-transfer properties of blue and purple copper proteins. Coordination Chemistry Reviews, 1999, **185-186** (1): 127～140

27 Fersht A R. Structure and Mechanism in Protein Science: A Guide to Enzyme Catalysis and Protein Folding. New York: W H Freeman & Company, 1999. 517

绿脓杆菌 apoazurin 在溶液中存在两种天然构象

钟 金[1,2] 张洪杰[1)*]

([1)]中国科学院生物物理研究所，北京 100101; [2)]吉林大学生命学院药学系，长春 130023)

摘要 如何解释绿脓杆菌 apoazurin 变性过程的复杂机制是一个有争议的问题. 最近的研究表明 apoazurin 的复杂变性机制可以归结为其天然态存在着至少两种构象. 利用内源荧光发射谱和圆二色谱进一步研究了 apoazurin 的脲变性机制，发现其稳态脲变性符合表观的二态过程，但其动力学为双相过程. 在高浓度脲中快反应在几秒钟内完成，而慢反应要经过几个小时. 快反应和慢反应的 m_u 值分别为 2.24 和 2.45 kJ·mol^{-1}·M^{-1}，去折叠活化能的差值为 22 kJ·mol^{-1}. 时间分辨的荧光发射谱和圆二色谱可以用天然态和完全变性态的谱图通过一个固定的比例参数进行重建. 结果表明，过去被广泛接受的存在着变性中间体的机制是不正确的，而 apoazurin 在天然态存在至少两种构象的假设是合理的.

关键词 *Pseudomonas aeruginosa* apoazurin，去折叠，荧光光谱，圆二色谱

学科分类号 Q51

* 通讯联系人. Tel: 010-64837257, Fax: 010-64872026, E-mail: hjzhang@sun5.ibp.ac.cn

收稿日期：2006-01-11，接受日期：2006-02-27